

## NUMERICAL MODEL STUDY OF TEMPERATURE DISTRIBUTIONS IN A HARBOUR

by

ROGER A. FALCONER<sup>1</sup>

### ABSTRACT

The paper gives details of a study to predict numerically the background temperature rise in Poole Harbour and Holes Bay, in Dorset, England, caused by the siting of either a 700MW or a 350MW power station. The numerical model is based on the numerical integration of the flow equations which simulate the water movements of tides and upon numerical integration of the advective-diffusion equation representing the movement of heat.

The results of the study predominantly suggest that the temperature field is proportional to the station capacity, with the maximum and mean temperatures across the basin for the 700MW station capacity being almost exactly double the corresponding values predicted for the 350MW station capacity. Observations from the velocity fields and tidal prism ratios both tend to suggest that Poole Harbour and Holes Bay have poor flushing characteristics, which confirm the relatively high temperature predictions in that only a relatively small volumetric percentage of the heated water is flushed out of the basin during each flood tide.

### INTRODUCTION

A two-dimensional numerical model has been developed to predict the depth average velocity fields and temperature distributions in narrow entranced harbours, within which a warm water outfall may be located. In a study for the Central Electricity Generating Board the model has been applied to Poole Harbour and Holes Bay, in Southern England, where the main objectives have been to determine the tide induced velocity fields and to make an assessment of the background temperature rise in the harbour as a result of a heated discharge from a power station having two possible capacities, i.e. either 700MW or 350MW. Water extracted from the entrance to Holes Bay, which is connected to the northern part of Poole Harbour and diametrically opposite the harbour entrance, flows through the condensers of the power station to be heated through 10K before being discharged back into

---

<sup>1</sup> Lecturer in Civil Engineering, University of Birmingham, Birmingham, England

the middle of Poole Harbour through a diffuser located approximately 500m south of the northern shoreline of the Harbour, see Fig.1.

The numerical model is based on the depth integration of the governing hydrodynamic equations which define the tidal water movements within the basin, and upon integration of the advective-diffusion equation representing the movement of heat. The geometry of Poole Harbour is of particular interest to the numerical modeller since the narrow entrance illustrated in Fig.1, gives rise to relatively large advective accelerations. Also, the plan wetted surface area of the harbour changes considerably throughout the tidal cycle, with the surface area at low tide being appreciably smaller than the corresponding surface area at high tide.

Other difficulties encountered in the numerical model study were the treatment of the open boundary conditions, particularly for temperatures at the seaward boundary on the flood tide, and also the simulation of the temperature discontinuity at the point source outfall.

GOVERNING EQUATIONS

The governing equations used in the numerical model to determine the water elevations, the depth averaged velocity components and the horizontal temperature variations in Poole Harbour were the two momentum equations, describing the fluid motion in the horizontal plane, and the equations of mass and heat balance. For a constant density turbulent fluid flow on a rotating earth, the depth integrated momentum equation for flow in the x-direction can be expressed as, (see Falconer (1976) and Goldstein (1938):-

$$\frac{\partial q_x}{\partial t} + \beta \left[ \frac{\partial Uq_x}{\partial x} + \frac{\partial Vq_x}{\partial y} \right] - fq_y + gH \frac{\partial \eta}{\partial x} + \frac{gq_x \sqrt{q_x^2 + q_y^2}}{H^2 C^2} - \epsilon \left[ 2 \frac{\partial^2 q_x}{\partial x^2} + \frac{\partial^2 q_x}{\partial y^2} + \frac{\partial^2 q_y}{\partial x \partial y} \right] = 0 \quad \dots (1)$$

and similarly for momentum conservation in the y-direction:-

$$\frac{\partial q_y}{\partial t} + \beta \left[ \frac{\partial Uq_y}{\partial x} + \frac{\partial Vq_y}{\partial y} \right] + fq_x + gH \frac{\partial \eta}{\partial y} + \frac{gq_y \sqrt{q_x^2 + q_y^2}}{H^2 C^2} - \epsilon \left[ \frac{\partial^2 q_y}{\partial x^2} + 2 \frac{\partial^2 q_y}{\partial y^2} + \frac{\partial^2 q_x}{\partial x \partial y} \right] = 0 \quad \dots (2)$$

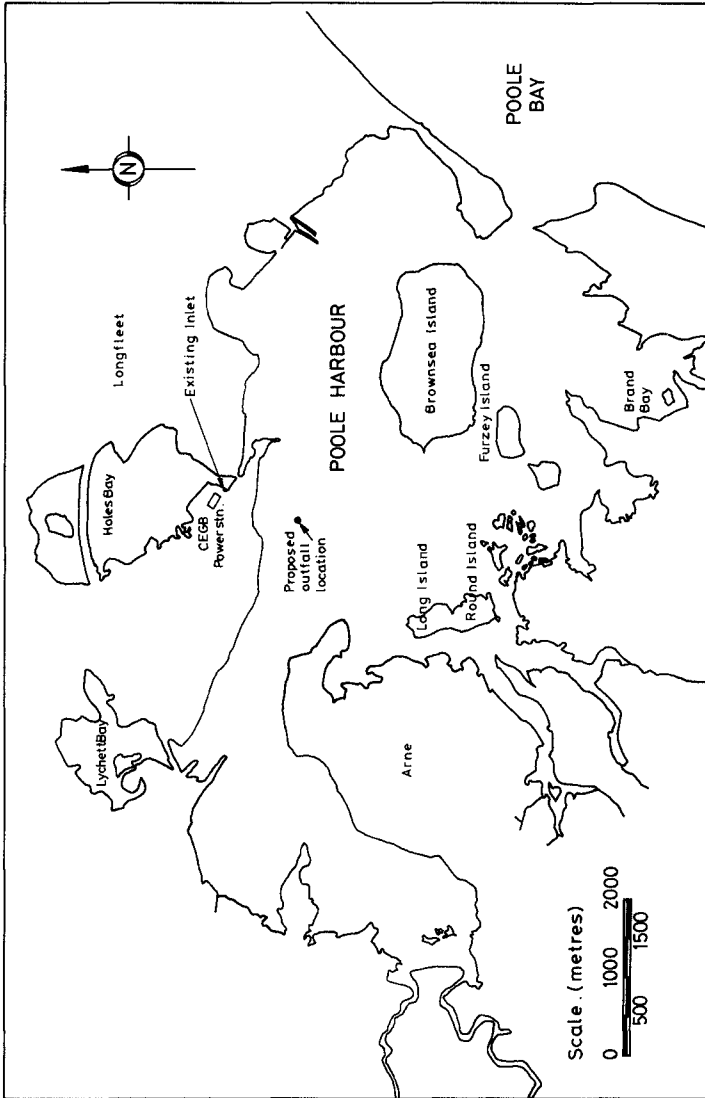


Fig. 1. Sketch of Poole Harbour and Holes Bay Showing Power Station Location.

where  $q_x$  and  $q_y$  = discharges per unit width in the x and y directions, with  $U$  and  $V$  being the corresponding depth averaged velocity components,  $\beta$  = a correction factor for the non-uniformity of the velocity distribution,  $H$  = total depth of flow,  $\eta$  = water surface elevation above chart datum,  $f$  = Coriolis parameter =  $2\omega\sin\phi$  where  $\omega$  is the angular velocity of the earth's rotation and  $\phi$  the geographical latitude (assumed to be  $50.012^\circ$ ),  $g$  = gravitational acceleration,  $C$  = Chezy's roughness coefficient =  $H^{2/3}/n$  where  $n$  is Manning's roughness coefficient (assumed to be 0.035) and  $\epsilon$  = depth mean eddy viscosity which, for an assumed logarithmic velocity profile in the vertical plane, becomes  $0.07\sqrt{g(q_x^2+q_y^2)}/C$ .

The depth integrated conservation equations for mass and heat transport can be expressed in a similar manner, giving for mass:-

$$\frac{\partial \eta}{\partial t} + \frac{\partial q_x}{\partial x} + \frac{\partial q_y}{\partial y} = 0 \quad \dots\dots (3)$$

and for heat, see Fischer (1978):-

$$\underbrace{\frac{\partial TH}{\partial t}}_{(1)} + \underbrace{\left[ \frac{\partial Tq_x}{\partial x} + \frac{\partial Tq_y}{\partial y} \right]}_{(2)} = \underbrace{- \frac{E(T-T_E)}{\rho Cp}}_{(3)}$$

$$+ \frac{(T_{IN} + \Delta T)Q_{OUT}}{A_{OUT}} + \underbrace{\frac{\partial}{\partial x} \left[ HD_{xx} \frac{\partial T}{\partial x} + HD_{xy} \frac{\partial T}{\partial y} \right] + \frac{\partial}{\partial y} \left[ HD_{xy} \frac{\partial T}{\partial x} + HD_{yy} \frac{\partial T}{\partial y} \right]}_{(5)} \quad \dots\dots (4)$$

where  $T$  = depth averaged temperature,  $E$  = surface heat exchange coefficient (assumed to be  $30W/m^2/K$ ),  $T_E$  = equilibrium temperature (assumed to be zero),  $\rho Cp$  = specific thermal capacity of fluid (assumed to be  $4.2MJ/m^3/k$  for water),  $T_{IN}$  = temperature at power station inlet,  $\Delta T$  = temperature rise across the condensers (assumed to be  $10K$ ),  $Q_{OUT}$  = discharge from the power station outlet (corresponding to  $23.4m^3/s$  for a 700MW power station and  $11.7m^3/s$  for a 350MW power station),  $A_{OUT}$  = plan cross-sectional area of outfall from power station and  $D_{xx}$ ,  $D_{xy}$ ,  $D_{yy}$  = depth averaged dispersion coefficients in the x, y, xx, xy, yy directions respectively, which have been shown by Preston (1981a) to be of the form:-

$$D_{xx} = \frac{(D_L q_x^2 + D_t q_y^2) \sqrt{g}}{\sqrt{q_x^2 + q_y^2} C} \quad D_{yy} = \frac{(D_L q_y^2 + D_t q_x^2) \sqrt{g}}{\sqrt{q_x^2 + q_y^2} C}$$

$$D_{xy} = D_{yx} = \frac{(D_l + D_t) q_x q_y \sqrt{g}}{\sqrt{q_x^2 + q_y^2} C}$$

where  $D_l$  and  $D_t$  are constants referring to the longitudinal dispersion and lateral diffusion components of the depth averaged dispersion coefficients and have assumed values of 5.93, after Elder (1959), and 0.15, after Fischer (1973), respectively for a logarithmic velocity profile. The numbered terms of the heat balance equation (4) refer to temperature variations within the domain as a result of : local effects (1), advective effects (2), net surface heat transfer (3), heat source such as an outfall (4) and turbulent diffusion and dispersion (5).

#### FINITE DIFFERENCE REPRESENTATION

The finite difference equations corresponding to the governing differential equations were expressed in an alternating direction implicit form with all terms being fully centred in both space and time, except for the pressure gradients in the momentum equations and the cross-product diffusion terms in the heat balance equation, see Falconer (1980 and 1981). The first order scheme, with accuracy  $O(\Delta t, \Delta x^2)$ , involved the discrete values of the variables being represented on a space staggered grid scheme in which water elevations and temperatures were described at different grid point locations to the discharges per unit width in the x and y directions.

The only terms requiring special mention are the advective accelerations expressing the lateral transport of momentum in the x and y directions of the momentum equation, e.g. the  $Vq_x$  product term in Eq.(1). These terms were represented in the finite difference scheme as for the Marker and Cell Technique so that their spatial locations were dependent upon the direction of the velocity components perpendicular to the axis direction being considered, see Williams and Holmes (1974).

The boundary conditions used for the hydrodynamic model of Poole Harbour included zero discharges per unit width perpendicular to the closed boundaries, with known uni-directional inflows being specified for the rivers and the power station throughflow. At the seaward boundary, just outside the harbour entrance, water elevation variations were assumed to vary in the same manner as for the mean spring and neap tidal curves given on the Admiralty Chart No.2611. The local discharge of heated water from the power station outlet was accounted for in the model by increasing the local water elevation in the mass conservation equation by an appropriate amount at the discrete point coinciding with the outfall.

For the heat balance equation the temperatures at the open boundaries also needed to be described as a function of time, together with the river inflow temperatures which were assumed to be zero at all times. At the outer seaward boundary, temperatures for the ebb tide were extrapolated linearly from values computed within the

computational field, as given by Leendertse and Gritton (1971). In this approximation only transport of heat by advection to the boundary was simulated, with dispersive heat transport assumed to be negligible. This method of determining the boundary temperature was also used to evaluate the temperature at the power station inlet, where flow was always in the outward direction across the boundary as for the ebb tide.

For the flood tide temperature variations at the open boundary PRESTON (1981b), in a study of the temperature variations at the mouth of Poole Harbour, suggested three possible methods for determining the governing temperatures. Of the possible representations given, the tidally averaged model was adopted due to its mathematical simplicity and relatively straightforward computational requirements. Based on a number of physical assumptions and assumed values for certain relevant data, Preston suggested that the boundary temperature could be expressed as:-

$$T(t) = \bar{\theta} \bar{T} \dots\dots (5)$$

where  $T(t)$  = tidal and spatially averaged input boundary temperature at time  $t$ ,  $\bar{\theta}$  = a tidally averaged integral function which, based on Preston's assumed data, had a value of 0.863, and  $\bar{T}$  = mean outflow temperature across the boundary, defined as:-

$$\bar{T} = \frac{\int_{t_1}^{t_2} \left[ \int_0^x q_x(t)T(t)dx + \int_0^y q_y(t)T(t)dy \right] dt}{\int_{t_1}^{t_2} \left[ \int_0^x q_x(t)dx + \int_0^y q_y(t)dy \right] dt}$$

where, for any tidal cycle,  $t_1$  and  $t_2$  = the initial and final times of ebb flow across the boundary and  $x$  and  $y$  = the open boundary lengths in the  $x$  and  $y$  directions respectively. Once the mean outflow temperature  $\bar{T}$  had been determined for the ebb tide, the corresponding value was used in Eq.(5) to give the mean boundary temperature during the subsequent flood tide.

The local discharge of heat from the power station outfall gave rise to a local temperature discontinuity, in that the fluid flowing through the warm water outfall grid squares underwent an abrupt temperature rise. This discontinuity gave rise to a series of spurious wave-type temperature oscillations across the harbour, occurring as a consequence of the inability of the finite difference technique to represent rapidly varying variables in space, see Leendertse and Gritton (1971).

In order to overcome the problem of spurious temperature predictions, a number of different numerical schemes were studied for the heat balance equation. The first method considered was Lax's method, see Lax (1954), in which the temperature at the lower time-step for the time derivative in the heat balance equation was expressed as the average of the temperatures at the four surrounding

grid points. However, although this scheme eliminated the spurious solutions, the method introduced an effective artificial diffusion coefficient into the heat equation which, for this study, was found to be intolerably large, see Falconer (1981).

The second scheme considered involved using upstream differencing for the advective terms, with the addition of an anti-diffusion term to improve on the initial poor accuracy of the scheme, as used by Miles (1980). However, this method was found to be unsatisfactory for this particular study since the anti-diffusion term either had to be removed fully or reduced near to the outfall, thereby appearing to introduce small amplitude temperature waves.

The final scheme studied, and subsequently adopted, involved treating the temperature discontinuity as a shock front, and thereby introducing just sufficient artificial diffusion to counteract the disturbances caused by the temperature discontinuity at the outfall. The artificial diffusion term was chosen so that the required additional diffusive effect was obtained when adjacent temperature values were widely different in the numerical model, but negligible when they were nearly equal, see Leendertse and Gritton (1971). Thus, added to the true diffusion terms in the heat balance Eq.(4) were two further diffusive terms of the form:-

$$D = \frac{\partial}{\partial x} \left[ HD_x \frac{\partial T}{\partial x} \right] + \frac{\partial}{\partial y} \left[ HD_y \frac{\partial T}{\partial y} \right] \dots\dots (6)$$

where the required diffusion coefficients are of the form:-

$$\left. \begin{aligned} D_{x_{j+\frac{1}{2},k}} &= \left[ \frac{T_{j+1,k} - T_{j,k}}{T_{j+1,k} + T_{j,k} - 2T_b} \right]^2 \left[ \frac{q_x \Delta x}{2} \right] \\ D_{y_{j,k+\frac{1}{2}}} &= \left[ \frac{T_{j,k+1} - T_{j,k}}{T_{j,k+1} + T_{j,k} - 2T_b} \right]^2 \left[ \frac{q_y \Delta y}{2} \right] \end{aligned} \right\} \dots\dots (7)$$

where j and k = grid point locations in the x and y directions respectively, and  $T_b$  = initial mean temperature, or base temperature, within the domain. Although the use of such an artificial diffusive term is by no means ideal in treating the temperature discontinuity arising at an outfall, the apparent advantage of this method is that the artificial diffusion falls off rapidly away from the outfall - where advection is often the dominant mode of heat transport.

In Poole Harbour large areas of shallow water exist such that marshes alternately dry and flood with each tidal cycle, and with much of the land-water boundary therefore being time dependent. In

simulating this moving boundary in the numerical model the procedure adopted was similar to that used by Leendertse and Gritton (1971), whereby the location of the land-water boundary was assumed to be a function of the current value of the depth. There were, however, two basic differences between Leendertse and Gritton's procedure and that used in this study. Firstly, the first and second checks in Leendertse and Gritton's method on whether or not a grid point should be dry were combined and carried out between the calculation for the new water elevation field and the temperature field. Also, only the two cross-sections in the implicit direction were considered rather than all four cross-sections for each grid square. Secondly, in the third check on a grid cell drying, the average water elevation was used in calculating each cross-section rather than just the water elevation at the grid point being considered. These changes allowed a reduction in the computational cost and appeared to reduce the influence of the instabilities generated in that the same cross-sections were used in these checks as in the finite difference equations themselves.

#### NUMERICAL MODEL APPLICATION AND RESULTS

The region of Poole Harbour and Holes Bay illustrated in Fig.1 was simulated in the numerical model using a finite difference mesh of  $65 \times 58$  grid points, with an equal grid spacing of 150m. At the centre of each grid square a representative depth between chart Datum and the bed was determined by equating the corresponding cross-sections in the numerical model to those defined by the actual bed topography. The tidal data required at the open seaward boundary was obtained from the Admiralty Chart No.2611 and data provided by the Poole Harbour Commissioners.

The cold water inlet to the power station was approximated by a horizontal sink, which was represented by an open boundary grid square of length 150m. For the proposed outfall, which was coincident with the centre of four grid squares, it was assumed that the heated fluid was discharged vertically upwards and that complete mixing occurred equally among the four adjacent grid squares. The advantage of using four rather than one grid square for the outfall, was that in discharging the heated water over a larger plan cross-sectional area a more realistic localised temperature field was predicted in the vicinity of the source itself. However, since heat rather than temperature was being conserved in the model, it was not surprising to find that when comparisons were made between using one and four grid cells to represent the outfall, little difference occurred in the predicted temperatures across the domain - except in the region very close to the outfall.

The model was always started at high tide, with the assumption that the initial velocities and temperatures were zero everywhere and that the outfall temperature rise above the intake temperature was 10K. Each simulation was run for a maximum of fourteen repetitive tidal cycles, a restriction placed on the model by the relatively small grid spacing and the stability requirement given by Falconer (1976 and 1980), i.e. that the time step  $\Delta t < \Delta x U$  - where  $U$  is the maximum depth averaged



velocity in the field and  $\Delta x$  the grid spacing (=150m). The resulting predicted water elevations, velocity components and temperatures were evaluated at each grid point, with the results being printed out in both numerical and graphical form at various phases of the tidal cycle.

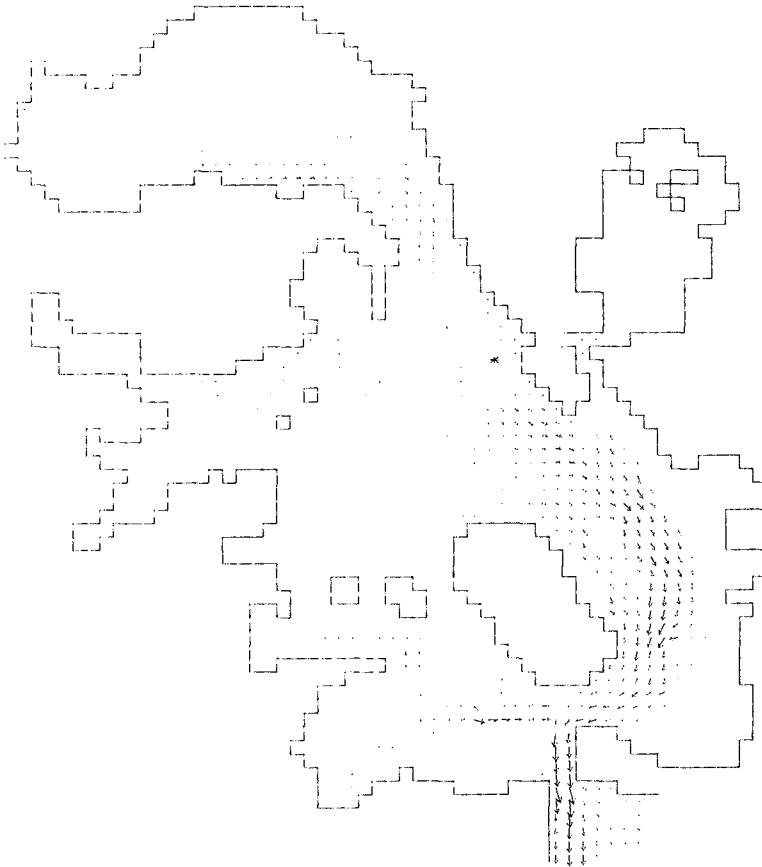
In general, it is always preferable to be able to check the predicted results obtained from a numerical model with field measurements or otherwise before proceeding with any analysis of the numerical results; the same being true for a laboratory model investigation. For this particular study it was not possible to make any worthwhile comparisons between any measured and predicted velocities or temperatures, since no appropriate field data was available at the time. However, since the model has been applied to a number of rectangular harbours with different aspect (or length to breadth) ratios and has been shown to give good agreement with scaled physical model results, see Falconer (1980), then it was assumed that the results obtained for this study ought not to differ markedly from any similar laboratory model investigations.

The velocity and temperature fields were reproduced graphically for four main simulations. These simulations included predictions for both a 700MW and a 350MW power station and for fourteen consecutive spring and neap tidal cycles respectively. The results are documented and compared in some detail in Falconer (1981), with some typical velocity and temperature field predictions being given in Figs. 2-5 for the spring tide simulations with a 350MW power station. Comparison of Figs. 2 and 3 gives an indication of the variation in the plan cross-sectional wetted area during the tidal cycle, and with the advective effect of the tide on the thermal plume being clearly illustrated in Figs. 4 and 5. Similarly, low neap tide results are given in Figs. 6 and 7.

In comparing the temperature predictions obtained for the various simulations, see Falconer (1981), it appears that the mean temperature and the standard deviation across the harbour were almost exactly double for the 700MW station capacity as for the 350MW capacity. For the 700MW power station the mean temperature rise across the harbour for the spring tides was 0.8K and with a standard deviation of 1.2K, whereas the corresponding values for the 350MW capacity were 0.4K and 0.6K respectively. Similarly, the corresponding neap tide predictions for the mean and standard deviations were 1.1K and 2.1K respectively for the 700MW station, and 0.6K and 1.1K for the 350MW station. The build-up of the mean temperature in the harbour during the fourteen tides for both the spring and neap tidal cycles is shown in Fig.8 for the 350MW power station. More recent numerical model studies on Poole Harbour by the Author, however, indicate that the temperatures predicted in this study might well be on the pessimistic side for two reasons. Firstly, the simulation of conditions in the harbour for fourteen identical neap tides means that a pessimistically low sequence of tidal ranges has been assumed over the period modelled, giving rise to a lower degree of flushing than would occur in reality. Secondly, the assumption that 86% of the heat discharged out through the open seaward boundary returns on the next flood tide appears to be conservative in comparison with recent field data measurements recorded

## VELOCITIES IN POOLE HARBOUR &amp; HOLES BAY

TIME = 168.20 HRS (LWL)



LENGTH SCALE = 150 M

AVERAGE DEPTH = 1.02 M

TIDAL RANGE = 1.98 M

VELOCITY → 1.00 M/S

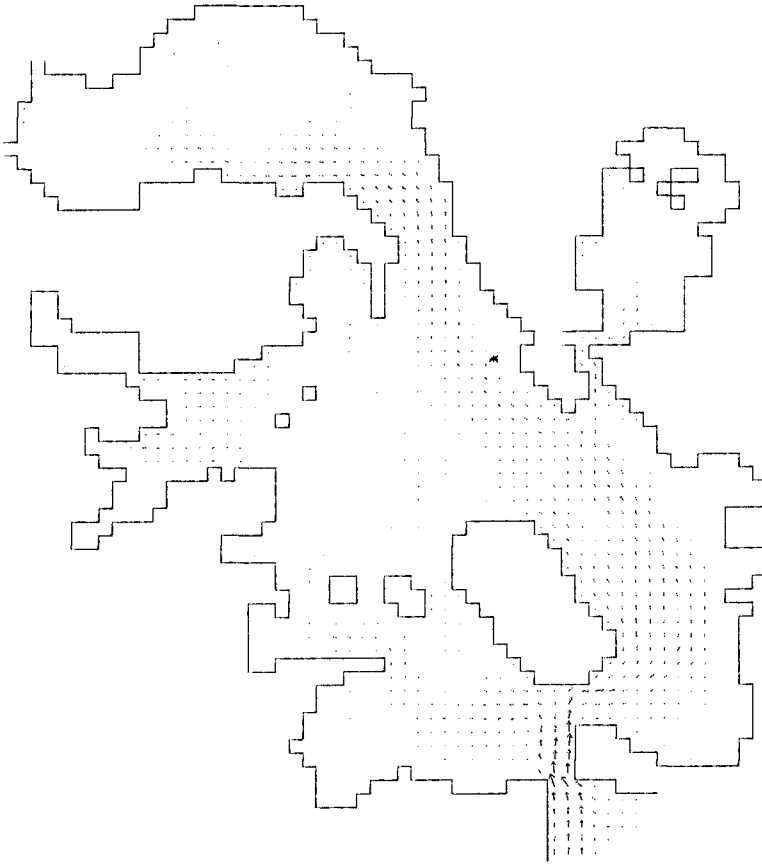
MANNING NUMBER = 0.035

TIDAL PERIOD = 12.4 HR

Fig.2. Velocities at low water spring tide for 350 MW power station

## VELOCITIES IN POOLE HARBOUR &amp; HOLES BAY

TIME = 173.00 HRS (HWL)



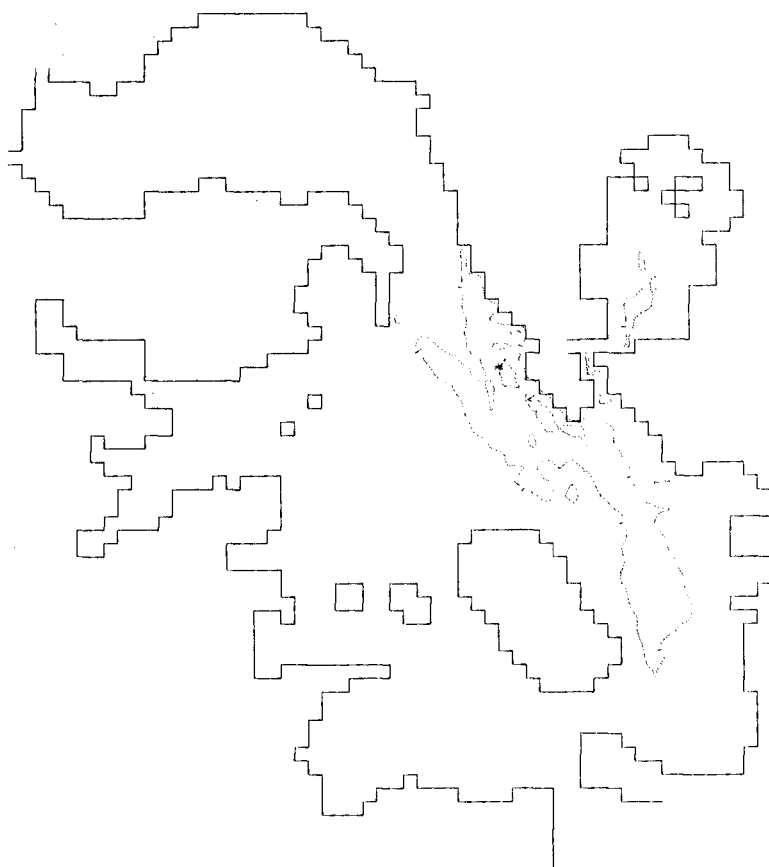
LENGTH SCALE = 150 M  
 AVERAGE DEPTH = 2.39 M  
 TIDAL RANGE = 1.90 M

VELOCITY → 1.00 M/S  
 MANNING NUMBER = 0.035  
 TIDAL PERIOD = 12.4 HR

Fig.3. Velocities at high water spring tide for 350 MW power station

## TEMPERATURES IN POOLE HARBOUR &amp; HOLES BAY

TIME = 168.20 HRS (LWL)



LENGTH SCALE = 150 M

MEAN VELOCITY = 0.19 M/MS

MEAN TEMP = 15.59 DEG K

ISOTHERMS = 0.5 DEG K

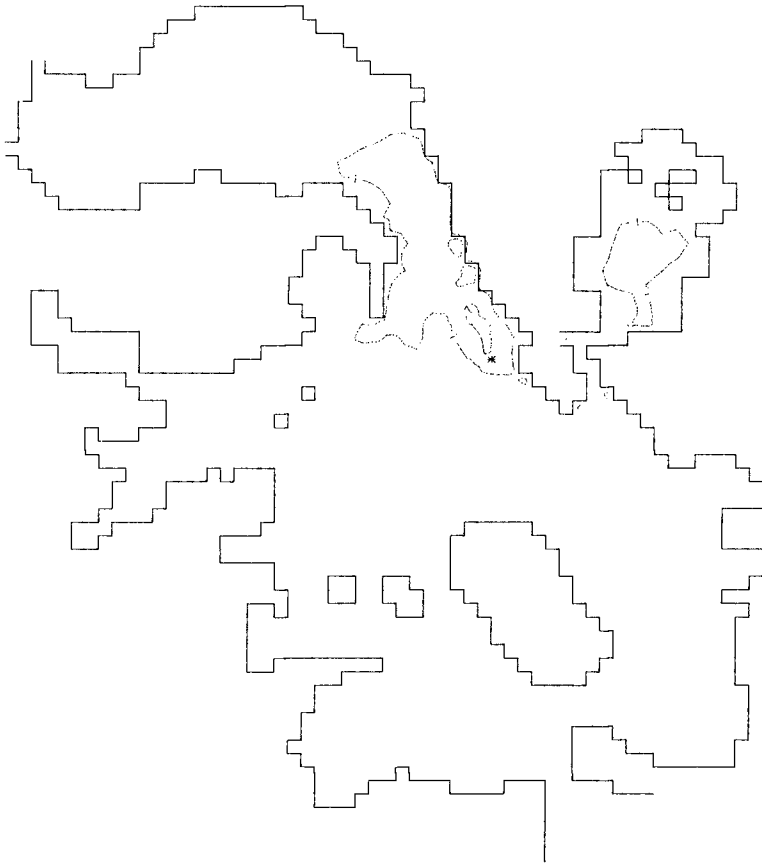
VEL. DEVIATION = 0.12 M/MS

TEMP. DEV. = 0.66 DEG K

Fig.4. Temperatures at low water spring tide for 350 MW power station

TEMPERATURES IN POOLE HARBOUR & HOLES BAY

TIME = 173.60 HRS (HWL)



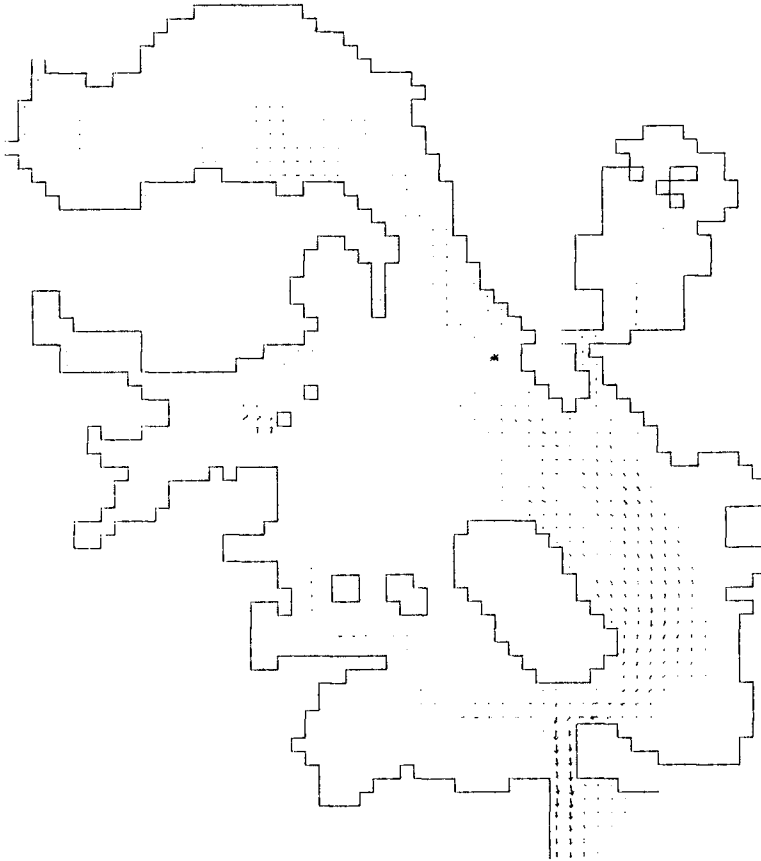
LENGTH SCALE — 150 M  
MEAN VELOCITY = 1.38 MM/S  
MEAN TEMP = .42 DEG K

ISOTHERMS ..... DEG K  
VEL. DEVIATION = 1.16 MM/S  
TEMP DEV = .60 DEG K

Fig.5. Temperatures at high water spring tide for 350 MW power station

## VELOCITIES IN POOLE HARBOUR &amp; HOLES BAY

TIME = 164.90 HRS (LWL)



LENGTH SCALE = 150 M

AVERAGE DEPTH = 1.97 M

TIDAL RANGE = .62 M

VELOCITY → 1.00 M/S

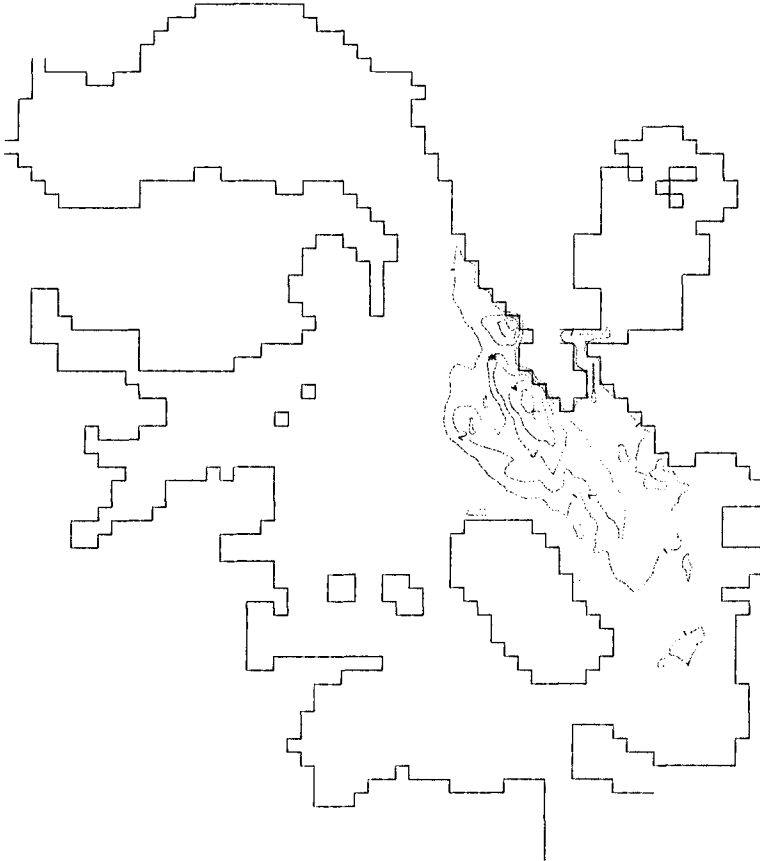
MANNING NUMBER = 0.035

TIDAL PERIOD = 12.4 HR

Fig.6. Velocities at low water neap tide for 350 MW power station

TEMPERATURES IN POOLE HARBOUR & HOLES BAY

TIME =164.80 HRS (LWL)



LENGTH SCALE — 150 M  
MEAN VELOCITY =100 MM/S  
MEAN TEMP = .68 DEG K

ISOTHERMS ----- DEG K  
VEL DEVIATION =114 MM/S  
TEMP DEV = 1.14 DEG K

Fig.7. Temperatures at low water neap tide for 350 MW power station

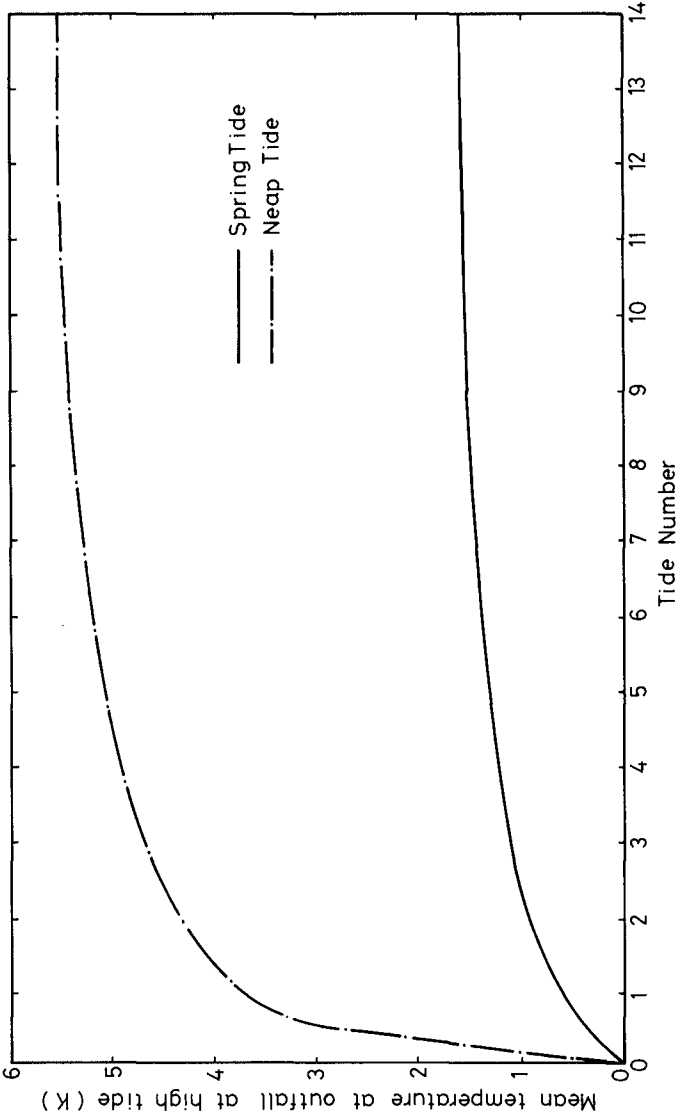


Fig.8. Variation of high tide mean temperature at the outfall with tide number.



for other substances such as nitrates and phosphates.

Other indications from the numerical model study were that Poole Harbour and Holes Bay both appear to have poor flushing characteristics, particularly for neap tides where results showed that the net tidally averaged heat outflow across the entrance was extremely small.

#### CONCLUSIONS

A numerical model has been developed which is capable of predicting both the velocity and temperature distributions within a narrow entranced harbour, with a heated discharge being located within the basin. The results obtained have proved to be encouraging, with numerically stable predictions having been obtained for relatively large advective accelerations and appreciable changes in the plan-form wetted area during the tidal cycle.

The numerical difficulties associated with the finite difference representation of the temperature discontinuity arising at the outfall have been overcome by a weighted artificial diffusive term, where the weighting factor is proportional to the square of the temperature difference between adjacent grid cells.

The results of the study show that for the 350MW power station the mean temperature rise across the harbour is 0.4K for spring tides and 0.6K for neap tides, with the standard deviations for the temperature fields being 0.6K and 1.1K respectively. The corresponding predictions made for the 700MW power station were, in almost all cases, exactly double the temperatures predicted for the 350MW station. However, for the reasons given in the previous section these predictions are thought to be on the conservative side.

#### ACKNOWLEDGEMENTS

The study was funded by the Central Electricity Generating Board under the supervision of Mr. I. T. Hughes, Station Planning Engineer. The author is also grateful for the assistance provided by Mr. N. Ames and Mr. N. P. Baldwin of the Central Electricity Generating Board, Mr. R. W. Preston of the Central Electricity Research Laboratories and Miss G. Vaisey of the Department of Civil Engineering, University of Birmingham.

#### REFERENCES

- ELDER, J.W. (1959). The Dispersion of Marked Fluid in Turbulent Shear Flow. *Journal of Fluid Mechanics*, Vol.5, part 4, pp.544-560.
- FALCONER, R.A. (1976). *Mathematical Modelling of Jet-Forced Circulation in Reservoirs and Harbours*. Ph.D. Thesis, University of London, pp.237.

- FALCONER, R.A. (1980). Modelling of Plan-Form Influence on Circulation in Harbours. Proceedings of the Seventeenth Coastal Engineering Conference, ASCE, Sydney, pp. 2726-2744.
- FALCONER, R.A. (1981). Numerical Model Study of Temperature Distributions in Poole Harbour and Holes Bay. Report for the Central Electricity Generating Board, pp.63.
- FISCHER, H.B. (1973). Longitudinal Dispersion and Turbulent Mixing in Open Channel Flow. Annual Review of Fluid Mechanics, Vol.5, pp. 59-78.
- FISCHER, H.B. (1978). On the Tensor Form of the Bulk Dispersion Coefficient in a Bounded Skewed Shear Flow. Journal of Geophysical Research, Vol.83, No.C5, pp. 2573-2375.
- GOLDSTEIN, S. (1938). Modern Developments in Fluid Dynamics. Oxford University Press, Vol.1, pp. 330.
- LAX, P.D. (1954). Weak Solutions of Non-Linear Hyperbolic Equations and their Numerical Computation. Communications on Pure and Applied Mathematics, Vol.7, pp. 159-193.
- LEENDERTSE, J.J. & Gritton, E.C. (1971). A Water-Quality Simulation Model for Well-Mixed Estuaries and Coastal Seas: Vol.11, Computation Procedures. The Rand Corporation, R-708-NYC, pp. 53.
- MILES, G.V. (1980). A Numerical Model for Background Temperature Fields. Report No. EX806, Hydraulics Research Station, Wallingford, pp. 44.
- PRESTON, R.W. (1981a). Representation of Dispersion in Turbulent Shear Flow. Private Communications, Central Electricity Research Laboratories, Leatherhead, Surrey, pp. 5.
- PRESTON, R.W. (1981b). The Temperature Variation at the Mouth of Poole Harbour. Private Communications, Central Electricity Research Laboratories, Leatherhead, Surrey, pp.41.
- WILLIAMS, J.W. & HOLMES, D.W. (1974). Marker-and-Cell Technique, a Computed Programme for Transient Stratified Flows with Free Surfaces. Report No.134, Hydraulics Research Station, Wallingford, pp. 54.

## NOTATION

$A_{OUT}$	= plan cross-sectional area of outfall from power station
$C$	= Chezy coefficient
$c_p$	= specific heat of fluid
$D_{xx}, D_{xy}, D_{yx}, D_{yy}$	= Combined depth averaged dispersion and diffusion coefficients in the two-dimensional plane
$D_l$	= longitudinal dispersion coefficient
$D_t$	= lateral turbulent diffusion coefficient
$E$	= surface heat exchange coefficient
$f$	= Coriolis parameter
$g$	= acceleration due to gravity
$H$	= total depth of fluid
$j, k$	= finite difference co-ordinates in x, y directions respectively
$q_x, q_y$	= discharges per unit width in x, y directions respectively
$Q_{OUT}$	= discharge from power station outlet
$t$	= time
$t_1, t_2$	= initial and final times of ebb flow across boundary
$T$	= depth averaged temperature at a grid point
$T_b$	= base temperature, or temperature at start of simulation
$T_E$	= equilibrium temperature for heat surface exchange
$\bar{T}$	= mean outflow temperature across the boundary
$T_{IN}$	= temperature at power station inlet
$U, V$	= depth averaged velocities in x, y directions respectively
$x, y$	= longitudinal and lateral co-ordinates in the horizontal plane
$X, Y$	= open seaward boundary length in the x, y directions
$\beta$	= correction factor for non-uniformity of vertical velocity profile
$\Delta t$	= time step
$\Delta T$	= temperature rise across condensers
$\Delta x$	= grid spacing
$\epsilon$	= depth mean eddy viscosity
$\eta$	= water surface elevation
$\bar{\theta}$	= tidally averaged integral function after Preston (1981b)
$\rho$	= density of fluid